

UNIVERSITÉ DU QUÉBEC À MONTRÉAL

UTILISATION DU [¹⁸F]FLUORO-ÉTHOXYBENZOVESAMICOL
([¹⁸F]FEOBV) AVEC LA TOMOGRAPHIE PAR ÉMISSION DE POSITRONS
(TEP) COMME MESURE *IN VIVO* DE LA PERTE NEURONALE
CHOLINERGIQUE CHEZ LE RAT.

MÉMOIRE
PRÉSENTÉ
COMME EXIGENCE PARTIELLE
DE LA MAÎTRISE EN PSYCHOLOGIE

PAR
MAXIME PARENT

DÉCEMBRE 2011

UNIVERSITÉ DU QUÉBEC À MONTRÉAL
Service des bibliothèques

Avertissement

La diffusion de ce mémoire se fait dans le respect des droits de son auteur, qui a signé le formulaire *Autorisation de reproduire et de diffuser un travail de recherche de cycles supérieurs* (SDU-522 – Rév.01-2006). Cette autorisation stipule que «conformément à l'article 11 du Règlement no 8 des études de cycles supérieurs, [l'auteur] concède à l'Université du Québec à Montréal une licence non exclusive d'utilisation et de publication de la totalité ou d'une partie importante de [son] travail de recherche pour des fins pédagogiques et non commerciales. Plus précisément, [l'auteur] autorise l'Université du Québec à Montréal à reproduire, diffuser, prêter, distribuer ou vendre des copies de [son] travail de recherche à des fins non commerciales sur quelque support que ce soit, y compris l'Internet. Cette licence et cette autorisation n'entraînent pas une renonciation de [la] part [de l'auteur] à [ses] droits moraux ni à [ses] droits de propriété intellectuelle. Sauf entente contraire, [l'auteur] conserve la liberté de diffuser et de commercialiser ou non ce travail dont [il] possède un exemplaire.»

TABLE DES MATIÈRES

LISTES DES FIGURES	iv
RÉSUMÉ	v
INTRODUCTION	1
RAT CHOLINERGIC DEFICITS AND [¹⁸ F]FEOBV	4
Abstract	4
1. Background	5
2. Methods	7
2.1 Imaging Procedures	7
2.2 Images Processing and Estimation of Binding Parameters	7
2.3 Regional Distribution	8
2.4 NBM Lesion Study	8
2.5 Aging Study	9
2.6 Statistical Analyses	9
3. Results	9
4. Discussion	10
4.1 Normal brain distribution of [¹⁸ F]FEOBV BP _{ND}	11
4.2 NBM lesion effects on the brain [¹⁸ F]FEOBV BP _{ND}	11
4.3 Aging effects on brain [¹⁸ F]FEOBV BP _{ND}	13

CONCLUSION	14
APPENDICE A: FIGURES	16
RÉFÉRENCES	21

LISTES DES FIGURES

Figure 1: [^{18}F]FEOBV distribution in controls (a) and regional effect of NBM lesions (b).	16
Figure 2: Average [^{18}F]FEOBV BP_{ND} maps in 7 young normal rats.	17
Figure 3: t-statistical maps [non-lesioned > NBM lesioned] representing cortical declines of the [^{18}F]FEOBV BP_{ND} following NBM lesion.....	18
Figure 4: Distribution of [^{18}F]FEOBV BP_{ND} declines following lesion of the NBM.	19
Figure 5: t-statistical maps [3 months > 18 months old rats] representing declines of [^{18}F]FEOBV BP_{ND} in the old rats..	20

RÉSUMÉ

Le [^{18}F]Fluoro-éthoxybenzovesamicol ([^{18}F]FEOBV) a été identifié comme étant un des agents radioactifs les plus prometteurs pour l'imagerie du transporteur vésiculaire de l'acétylcholine en utilisant la tomographie par émission de positrons (TEP). Nous rapportons ici que cette approche est en mesure de détecter de subtiles pertes de terminaux cholinergiques, comme celles associées avec le vieillissement ou suivant la lésion partielle du noyau basal de Meynert (NBM). Vingt-et-un rats adultes ont été distribués également en trois groupes : 1) Rats âgés (18 mois); 2) Jeunes rats (3 mois); et 3) Rats avec une lésion unilatérale du NBM induite par une infusion locale de saporine-IgG 192. Pour les rats normaux et ceux avec lésion, la plus haute valeur de liaison du [^{18}F]FEOBV a été observée dans le striatum, suivi de valeurs similaires dans le cortex frontal et le thalamus, puis de valeurs plus faibles pour les hippocampes et le cortex temporo-pariétal. Les rats avec lésion du NBM ont démontré une liaison de [^{18}F]FEOBV diminuée principalement dans la partie ventrale du cortex frontal. Cette perte est plus importante du côté de la lésion, mais également présente dans la région homologue de l'hémisphère controlatéral. Le vieillissement a entraîné une diminution de liaison de [^{18}F]FEOBV localisée dans les hippocampes. Le [^{18}F]FEOBV semble être un marqueur très prometteur pour la quantification *in vivo* du transporteur vésiculaire de l'acétylcholine dans le cerveau; l'imagerie TEP avec cet agent permet la détection de réductions physiologique et pathologique de la densité des terminaisons cholinergiques.

Mots-clés : Tomographie par émission de positrons; transporteur vésiculaire de l'acétylcholine; neurodégénérescence; vieillissement; saporine-IgG 192; [^{18}F]Fluoro-éthoxybenzovesamicol

INTRODUCTION

L'acétylcholine (ACh) est un neurotransmetteur bien connu des systèmes nerveux périphérique (SNP) et central (SNC). Dans le SNC, les systèmes cholinergiques sont connus pour être impliqués dans la régulation de l'éveil et du sommeil paradoxal (Szymusiak, 1995), dans divers comportements liés à la motivation (Olmstead et Franklin, 1993) et dans certaines fonctions cognitives telles la mémoire et l'attention (Everitt et Robbins, 1997 ; Levin et Simon, 1998 ; Voytko, 1996). Les fonctions cognitives impliqueraient plus particulièrement un groupement de cellules cholinergiques localisé dans le Noyau Basal de Meynert (NBM), au niveau du prosencéphale basal, qui projette massivement au néocortex. La destruction partielle ou totale du NBM affecte négativement la performance de rats à diverses tâches d'attention visuelle (McGaughy *et al.*, 2002 ; Muir, Everitt et Robbins, 1994 ; Muir *et al.*, 1993).

Chez l'humain, le NBM est sévèrement touché dans la Maladie d'Alzheimer (MA), (Whitehouse *et al.*, 1982), et cette atteinte constitue l'indicateur neuropathologique le mieux corrélé avec la symptomatologie clinique (Dickson *et al.*, 1995 ; Dournaud *et al.*, 1995 ; Prohovnik *et al.*, 2006). Une telle atteinte du NBM s'observe également dans plusieurs autres maladies dégénératives du SNC comme la Maladie de Parkinson ou la démence à corps de Lewy (Whitehouse *et al.*, 1983). Ces deux maladies se caractérisent aussi par l'atteinte d'un autre groupement de cellules cholinergiques situé au niveau du tronc cérébral : les noyaux tegmentaire pédonculopontin (NTPP) et latéro-dorsal (NTLD), projetant principalement vers le thalamus et autres structures sous-corticales. Le NTPP s'avère touché de façon plus

sélective encore dans des maladies comme la dégénérescence cortico-basale, la dégénérescence striatonigrale, et la paralysie supranucléaire progressive (Henderson *et al.*, 2000 ; Hirano *et al.*, 2010). Cependant, on connaît mal le rôle précis de ces lésions cholinergiques dans ces maladies.

D'autres atteintes cholinergiques seraient aussi observées avec le vieillissement normal chez l'animal. Un groupement de cellules cholinergiques issues des noyaux du septum médian et projetant aux hippocampes montrerait des modifications morphologiques caractérisées par une réduction de la richesse des fibres cholinergiques. Cette réduction est exprimée par une réduction des marqueurs cholinergiques (Canas *et al.*, 2009) et de la longueur moyenne de ces fibres (Ypsilanti *et al.*, 2008).

La relation existante entre l'état des systèmes cholinergiques et diverses manifestations cliniques ou physiologiques a principalement été étudiée à partir de mesures *post-mortem*, comme des techniques immunohistochimiques. Un marqueur sélectif d'une composante structurelle ou métabolique des neurones cholinergiques sert ainsi de sonde pour identifier, quantifier et déterminer l'intégrité des cellules. Il est également possible de procéder à de telles mesures *in vivo*, à partir de marqueurs pouvant être détectés par imagerie cérébrale. Les traceurs radioactifs avec la Tomographie par Émission de Positrons (TEP) sont d'excellents candidats pour ces mesures. Ces traceurs sont composés d'un ligand spécifique à un site synaptique et d'une queue radioactive qui génère des émissions β^+ (dégradation des protons du noyau atomique en positrons). L'annihilation encourue par l'impact de chaque positron avec un électron du milieu génère deux rayons gamma émis en directions opposées. En captant et en analysant la trajectoire de ces rayons, on peut en déduire la concentration du traceur dans différents sites cérébraux.

Présentement, il existe certains marqueurs dont le ligand se fixe à l'acétylcholinestérase (AChE), l'enzyme de dégradation extracellulaire de l'acétylcholine. On sait toutefois que la quantité d'AChE peut varier selon plusieurs conditions normales ou pathologiques et qu'il ne peut donc pas marquer la cellule

cholinergique proprement dite. D'autres marqueurs plus directs de la cellule cholinergique sont donc en cours de développement. La plus grande partie de ces traceurs sont des dérivés de la drogue vésamicol (Efange, 2000), et se lient de manière sélective au transporteur vésiculaire de l'acétylcholine, une protéine située dans la terminaison pré-synaptique des neurones cholinergiques. Parmi ceux-ci, notre équipe de recherche s'est attardée à développer le [^{18}F]Fluoro-éthoxybenzovesamicol ([^{18}F]FEOBV) (Kilbourn *et al.*, 2009 ; Landry St-Pierre *et al.*, 2008a), dont les caractéristiques physicochimiques et métaboliques sont des plus prometteuses (Giboureau *et al.*, 2010). Il montre une excellente affinité et une grande spécificité pour le transporteur vésiculaire de l'ACh (Mulholland, *et al.*, 1998). Ses propriétés pharmacocinétiques sont avantageuses et il ne produit aucun métabolite sanguin radioactif pouvant interférer avec les données d'imagerie cérébrale (Landry St-Pierre *et al.*, 2008b ; Mulholland *et al.*, 1998 ; Soucy *et al.*, 2010).

Jusqu'à maintenant, l'imagerie cérébrale avec le [^{18}F]FEOBV a montré, chez le rat comme chez le primate, une bonne capacité à se lier aux structures cérébrales riches en projections cholinergiques (Kilbourn *et al.*, 2009 ; Landry St-Pierre *et al.*, 2008a ; Soucy *et al.*, 2010). Il reste cependant beaucoup à déterminer avant de pouvoir penser à l'utiliser dans un contexte clinique chez l'humain. Avant toute chose, il faut déterminer si la mesure de liaison du [^{18}F]FEOBV est capable de détecter des altérations plus ou moins importantes des systèmes cholinergiques. Dans ce but, la présente étude vise à établir le profil de liaison du [^{18}F]FEOBV dans deux cas d'altérations des systèmes cholinergiques centraux chez le rat : 1) Suite à une lésion expérimentale du NBM, ainsi que 2) Lors du vieillissement normal.

RAT CHOLINERGIC DEFICITS AND [¹⁸F]FEOBV

Abstract

[¹⁸F]fluoroethoxybenzovesamicol ([¹⁸F]FEOBV) has been shown to be one of the most promising radioligands for imaging the vesicular ACh transporter (VACHT) with Positron Emission Tomography (PET). We report here that this approach can detect subtle cholinergic terminals losses such as those associated with aging, or those following a partial lesion of the nucleus basalis magnocellularis (NBM). Twenty-one adult rats were evenly distributed in three groups including 1) Aged rats (18 months); 2) Young rats (3 months); and 3) Rats with unilateral lesion of the NBM, following a local stereotaxic infusion of 192 IgG-saporin. In both normal and lesioned rats, our results revealed the highest [¹⁸F]FEOBV binding to be in the striatum, followed by similar values in both frontal cortex and thalamus, while lower values were observed in both hippocampus and temporo-parietal cortex. In the lesioned rats, [¹⁸F]FEOBV binding was found to be reduced mostly in the ventral frontal cortex on the side of the lesion, but some reduction were also observed in the homologous region of the contralateral hemisphere. Aging was found to be associated with a [¹⁸F]FEOBV binding reduction limited to the hippocampus of both hemispheres. [¹⁸F]FEOBV appears to be a very promising marker for the *in vivo* quantification of the brain VACHT; PET imaging of this agent allows *in vivo* detection of both physiological and pathological reductions of cholinergic terminals density.

1. Background

Cholinergic neurotransmission plays a key role in numerous and varied functions, from cognition to regulation of autonomic systems. Presynaptic components of the cholinergic neurons such as choline acetyltransferase (ChAT) and vesicular acetylcholine transporter (VACHT) are recognized markers of those cells, which are vulnerable targets of the aging process and of many neurodegenerative conditions (Mufson *et al.*, 2008 ; Quirion, 1993). For instance, loss of presynaptic cholinergic terminals constitutes an early aspect of the neuropathological process present in Alzheimer's Disease (AD), as well as in Progressive Supranuclear Palsy (PSP), and other Parkinsonian syndromes. *Post-mortem* studies have shown that cholinergic markers depletion strongly correlates with symptoms severity in AD (Dournaud *et al.*, 1995 ; Prohovnik *et al.*, 2006).

There is currently a lack of radiolabelled imaging agents for the *in vivo* quantification of cholinergic deficits. The need for such a tool is regularly emphasized (Thal *et al.*, 2006 ; Ward, 2007) as a potential biomarker for AD and other neurodegenerative diseases. Current imaging agents for the brain cholinergic systems provide information on a wide range of acetylcholine receptors as well as on its synthesizing enzyme, but those remain indirect surrogate markers of the cholinergic fibers *per se*. Direct imaging of the presynaptic cholinergic terminals is still a challenge in nuclear medicine, although some radiolabeled compounds have been studied with uneven successes.

Vesamicol may be considered as the best radiotracer precursor studied until now for quantifying VACHT (Efange, 2000). Amongst vesamicol derivatives for *in vivo* imaging, [¹⁸F]fluoroethoxybenzovesamicol ([¹⁸F]FEOBV) was found to be the most promising agent for the purpose of imaging VACHT with Positron Emission Tomography (PET). It displays fast kinetics, readily crosses the blood brain barrier, and binds with high affinity and selectivity to VACHT (Mulholland *et al.*, 1998). In

addition, peripheral [^{18}F]FEOBV metabolism does not generate metabolites capable of crossing the blood-brain barrier (Landry St-Pierre *et al.*, 2008b). [^{18}F]FEOBV is also stable in the brain and plasma, and does not generate significant amounts of free [^{18}F] in primates, as opposed to other vesamicol derivatives (Giboureau *et al.*, 2007 ; Kilbourn *et al.*, 2009 ; Soucy *et al.*, 2010). VAcHT may be quantified using reference tissue models due to its absence in the cerebellum (Ichikawa *et al.*, 1997). VAcHT has previously been imaged in the living human brain with using Single Photon Emission Computed Tomography (SPECT) and [^{123}I]IBVM, a radio-iodinated benzovesamicol analog. However, quantification on VAcHT using [^{123}I]IBVM is complex due to its slow kinetics and other quantification issues (Mazere *et al.*, 2008).

PET [^{18}F]FEOBV has demonstrated VAcHT concentrations present in discrete cholinergic projections of the brain in both rodents (Mulholland *et al.*, 1998) and primates (Kilbourn, *et al.*, 2009; Soucy, *et al.*, 2010). The highest binding has been invariably found to be in the striatum, corresponding to the local cholinergic interneurons (Mesulam *et al.*, 1992). Significant [^{18}F]FEOBV binding has also been detected in the cortex, the hippocampus and the thalamus, corresponding to projections arising respectively from the nucleus basalis of Meynert (NBM), the septal area, and the pontomesencephalic cholinergic nuclei (Mesulam *et Geula*, 1988 ; Mesulam *et al.*, 1989 ; Mesulam *et al.*, 1983). These data have been obtained in normal subjects, but the potential clinical applications of [^{18}F]FEOBV would rest mainly on its ability to detect VAcHT changes in the living brain. How sensitive is [^{18}F]FEOBV in detecting the slight cholinergic decline associated with aging, or the specific topographic denervation associated with a lesion of a cholinergic nucleus, remains to be established, and the current study addresses those questions.

We hypothesized that decreases in binding of the radioligand to VAcHT will be observed both in rats with a NBM lesion and in aged rats, when compared with controls. NBM lesions should result in a [^{18}F]FEOBV binding reduction in specific neocortical subregions (Pizzo *et al.*, 1999), whereas in aged rats [^{18}F]FEOBV binding should be reduced more diffusely in allocortical areas (Ypsilanti *et al.*, 2008).

2. Methods

All experiments followed the Canadian Council on Animal Care guidelines. Twenty-one adult male Long-Evans rats were used for this study. They were evenly distributed in three groups of 1) Old rats, average age of eighteen months (750-800 grams); 2) Young rats, average age of three months (250-300 grams); and 3) Rats with unilateral lesion of the NBM (average age of 3 months, 250-300 grams). All rats were housed under standard conditions in a 12h-12h light-darkness cycle, with *ad libidum* access to water and food.

2.1 Imaging Procedures

All rats (n = 21) were scanned using a CTI Concorde R4 microPET for small animals. Each PET session consisted in a five min. transmission followed by a 60 min. emission scan. PET scans were conducted under light isoflurane anesthesia (2% in medical air) delivered by a nose cone. Temperature, heart rate and blood pressure were monitored throughout the procedure using a BIOPAC system. The transmission scan was obtained using a rotating [^{57}Co] point source. Emission scans were initiated immediately after the transmission scan with a bolus injection of 11.1 to 18.5MBq (SA = 6152 Ci/mmol) of [^{18}F]FEOBV (Mzengeza *et al.*, 2007) administered in the tail vein. Transmission and emission scans were obtained using list mode acquisition. Images were histogrammed into 27 sequential time frames of increasing duration (8x 30sec, 6x 1min, 5x 2mins, 8x 5mins) over the 60 min. duration of the acquisition. Images were reconstructed using a *Maximum A Posteriori* (MAP) algorithm, normalized and corrected for scatter, dead time and decay.

2.2 Images Processing and Estimation of Binding Parameters

Imaging analysis was conducted using minctools (<http://www.bic.mni.mcgill.ca/ServicesSoftware/HomePage>). All images were

manually co-registered to a standard rat histological template (Rubins *et al.*, 2003) using a rigid body transformation. Binding Potential (BP_{ND}) was calculated using the graphical linearization reference-tissue method (Logan *et al.*, 1990) with the cerebellar cortex as reference tissue. Cerebellar time-activity curves for calculation of BP_{ND} were extracted by applying the rat cerebellum template to the dynamic activity maps. The resulting BP_{ND} images were convolved using a Gaussian kernel (FWHM = 0.6). Images were then normalized to their global BP value to account for inter-individuals differences.

2.3 Regional Distribution

In order to quantify [^{18}F]FEOBV distribution in the rat brain, volumes of interest (VOI) were traced on a standard histological template: 1) Frontal cortex; 2) Temporo-parietal cortex ; 3) Striatum; 4) Hippocampus, and 5) Thalamus. The populational regional BP_{ND} of all seven young non-lesioned rats was computed for each of these VOIs.

2.4 NBM Lesion Study

Immunocytotoxic lesions of the NBM were induced in one group of seven young rats using unilateral (left hemisphere) stereotaxic injection of the cholinergic neurons-selective immunotoxin 192 IgG-saporin (Pizzo *et al.*, 1999). Animals were first placed in a stereotaxic frame, following a brief anesthetic induction with 5% isoflurane administered in an induction chamber. During the stereotaxic procedures, anesthesia was maintained with 2% isoflurane. 192 IgG-saporin (*Advanced Targeting Systems*, lot 64-124) was infused with a microsyringe in the NBM (0.2 μ g dissolved in 0.2 μ L (n = 3), or 0.25 μ g in 0.5 μ L (n = 4)). The stereotaxic coordinates, taken from Paxinos & Watson (2009), were the following: 1mm posterior to bregma, 2.8mm lateral to midline, and 7.6mm ventral to cranium surface (n = 5), or 0.5mm, 2mm and 8.5mm (n = 2). During the two weeks following the surgery, no other experimentation was done with these rats in order to allow a full recovery.

2.5 Aging Study

Aging effects on the cholinergic systems were estimated cross-sectionally in the group of 18 months-old rats ($n = 7$; all males; average weight of 800g). These animals were only used for this experiment.

2.6 Statistical Analyses

Regional brain differences in the non-lesioned young rats ($n = 7$) were estimated across the five VOIs using one-way Analysis of Variance (ANOVA). Differences between the lesioned ($n=7$) and all non-lesioned rats ($n=14$) rats were assessed using both VOIs and voxel-based analyses, via one-way ANOVAs with age as covariate. The threshold for significance for VOI analysis was $p = 0.05$, after correction for multiple comparisons. The threshold for significance of the voxel level analysis was set at $t = 3.5$ ($p = 0.002$) for clusters of at least 100 contiguous voxels. In order to evaluate group effect in a significant cluster, BP_{ND} was averaged in voxels with t -values greater than 50% of the local maxima. The variability of NBM lesions was assessed by computing the probabilistic distribution of low [^{18}F]FEOBV BP_{ND} in the lesioned rats ($n = 7$). Individual binary maps representing declines of [^{18}F]FEOBV BP_{ND} (z -score > 2) were compiled into a probabilistic map. Individual z -scores were obtained based on statistical values obtained from non-lesioned animals. Comparisons between the young non-lesioned rats ($n = 7$) and the old rats ($n = 7$) were conducted at the voxel level using t -statistic analysis (Rminc, <https://launchpad.net/rminc>). The threshold for significance was $t = 3.5$ ($p = 0.004$) for clusters of at least 100 contiguous voxels.

3. Results

Regional distribution of [^{18}F]FEOBV BP_{ND} in the young normal rats (see Figure 1) shows a significant effect of VOI; $F(4, 13) = 14.44$, $p < 0.0005$. Highest

activity was found in the striatum ($p < 0.001$), followed by frontal cortex or thalamus ($p < 0.001$) and lastly by the hippocampus or temporo-parietal cortex ($p < 0.01$). Figure 2 shows this BP_{ND} distribution on the brain surface, together with selected slice examples.

Rats with lesions of the NBM showed a regional anatomical distribution of [^{18}F]FEOBV BP_{ND} , similar to that observed in young normal rats as revealed by the absence of significant difference for any VOI between the two groups. In contrast, voxel-based analysis showed a large cluster in the left ventral portion of the frontal cortex (from the anterior commissure: $x = -3.56\text{mm}$, $y = 1.24\text{mm}$, $z = -0.18\text{mm}$, $k = 41.88\text{mm}^3$), with a mean BP_{ND} of 1.33 ± 0.04 in controls, and 1.14 ± 0.05 in the lesioned rats ($t = 6.5$, $p < 0.0005$, $d = 4.2$; Figure 3). In the homologous region of the contralateral (right) hemisphere, a similar but smaller cluster was found ($x = 4.3\text{mm}$, $y = 0.89\text{mm}$, $z = -1.1\text{mm}$, $k = 23.34\text{mm}^3$). The BP_{ND} mean value in the contralateral cluster was 1.36 ± 0.03 in controls, and 1.18 ± 0.05 in the lesioned rats ($t = 5.6$, $p < 0.0005$, $d = 4.37$; Figure 3). The probabilistic distribution of abnormal [^{18}F]FEOBV BP_{ND} revealed a large variability of NBM lesions effects (see Figure 4).

Comparisons between young and aged rats showed significant [^{18}F]FEOBV BP_{ND} declines in the hippocampi of the old rats, for both the left ($x = -5.59\text{mm}$, $y = -6.13\text{mm}$, $z = 1.31\text{mm}$, $k = 13.44\text{mm}^3$) and right ($x = 5.58\text{mm}$, $y = -5.01\text{mm}$, $z = -0.98\text{mm}$, $k = 11.2\text{mm}^3$) hemispheres (see Figure 5). The average BP_{ND} in these clusters were 1.13 ± 0.04 and 1.03 ± 0.03 ($t = 7.2$, $p = 0.0005$, $d = 2.83$) in young and old rats, respectively.

4. Discussion

The present study has established the quantitative regional distribution of [^{18}F]FEOBV BP_{ND} in the rat telencephalon using PET with a bolus injection and reference tissue method. In addition, a [^{18}F]FEOBV BP_{ND} decline was described for the first time following both a unilateral cholinergic lesion of the NBM and as a result of aging.

4.1 Normal brain distribution of [^{18}F]FEOBV BP_{ND}

Our results indicate high [^{18}F]FEOBV BP_{ND} in the striatum, frontal cortex and thalamus, with lower values in the hippocampus and temporo-parietal cortex. This distribution pattern is in agreement with published values for concentrations of VAcHT, known to be associated with cholinergic terminals (Gilmor *et al.*, 1996 ; Ichikawa *et al.*, 1997 ; Weihe *et al.*, 1996). That distribution pattern is also consistent with that found in other immunohistochemistry studies targeting presynaptic cholinergic markers such as ChAT and VAcHT, as well as with previous PET imaging studies with [^{18}F]FEOBV (Fuhrmann *et al.*, 1985 ; Landry St-Pierre *et al.*, 2008a ; Mulholland *et al.*, 1998). Such a good agreement between our measurements of [^{18}F]FEOBV BP_{ND} and the literature supports the view that PET imaging with [^{18}F]FEOBV is a valid technique to measure cholinergic presynaptic terminal density in living individuals. The high striatal [^{18}F]FEOBV BP_{ND} most likely corresponds to the numerous terminals of the ACh containing mid spiny interneurons. In the thalamus, it probably depicts the well known cholinergic terminals arising from the pendunculo-pontine and latero-dorsal tegmental nuclei. In the cortex the greatest [^{18}F]FEOBV BP_{ND} was observed in the medial prefrontal area, which receives the densest cholinergic afferents from the NBM. Although regions of significant binding were also observed in the brainstem, these areas were not within the scope of the present study.

4.2 NBM lesion effects on the brain [^{18}F]FEOBV BP_{ND}

The BP_{ND} outcome used in this study expresses the ratio between tissue receptor density (B_{max}), and [^{18}F]FEOBV dissociation constant (K_D) (Innis *et al.*,

2007). Therefore, we believe that low BP_{ND} values observed in the rats with unilateral NBM lesions reflect a reduced tissue concentration of VAcChT. Although a low BP_{ND} could also result from an increased [^{18}F]FEOBV K_D , such an explanation remains unlikely if we consider that very little cholinergic markers can usually be observed in tissue after lesions with 192 IgG-saporin (Pizzo *et al.*, 1999). Alternatively, a decline in regional cerebral blood flow may have been induced in our rats by the cholinergic lesions (Kovalenko et Matsievskii, 2005). However, it is difficult to estimate the impact of these changes using reference tissue analyses.

The statistical clusters representing declines of [^{18}F]FEOBV BP_{ND} following the immunolesions were located in the ventral part of the frontal cortex. These areas were diffuse and heterogeneous enough that they were not statistically detected using a VOI method. This may be explained, at least in part, by variability in the 192 IgG-saporin doses and infusion sites, resulting in variable cortical denervation. Such an explanation is reinforced by the large variance of presynaptic cholinergic depletion depicted by the probabilistic lesion map shown in figure 4.

Bilateral infusion of 192 IgG-saporin in the NBM have previously shown clear but variable ChAT reductions in the cortex, with decreases ranging from 42 to 70% (Risbrough, Bontempi et Menzaghi, 2002). Unilateral lesions with similar 192 IgG-saporin doses also produce a ChAT reduction, with depletions ranging from 25 to 31% (Wenk *et al.*, 1994). Such a discrepancy might be present because the effects of a unilateral lesion are typically measured by comparing the lesioned hemisphere with the non-lesioned one. Our results suggest that the hemisphere contralateral to the lesion may not be an adequate control, as significant [^{18}F]FEOBV BP_{ND} decreases were observed on both sides. The smaller contralateral cluster of decrease indicates a possible fiber crossover in NBM projections to the cortex.

Our results with the lesioned rats suggest that [^{18}F]FEOBV may be useful to detect cortical cholinergic denervations such as those known to be present in AD or dementia with Lewy Bodies (DLB) (Dournaud *et al.*, 1995 ; Prohovnik *et al.*, 2006). However, further studies are needed to evaluate the reliability of this detection when

compared to *post-mortem* immunohistochemistry standards. In addition, it remains to be seen whether [^{18}F]FEOBV can detect lesions in other areas, such as those of the pontine cholinergic projections to the thalamus, known to occur in DLB as well as in PSP (Henderson *et al.*, 2000 ; Hirano *et al.*, 2010).

4.3 Aging effects on brain [^{18}F]FEOBV BP_{ND}

Aging effects on cholinergic neurotransmission have been extensively investigated in human brain tissue as well as in animal models with diverse results and interpretations. While postsynaptic cholinergic receptors are often shown to be sensitive to aging (Podruchny *et al.*, 2003), there is no consensus regarding the effect on presynaptic markers (Sherman et Friedman, 1990).

Our results supporting a bilateral and symmetric aging-related depletion of cholinergic innervation in the hippocampus are consistent with previous studies showing fiber length reduction (Ypsilanti *et al.*, 2008) or decrease of VAcHT in the hippocampus of 18 and 24 months old rats (Canas *et al.*, 2009). The age-related [^{18}F]FEOBV BP_{ND} decrease limited to the hippocampus suggests that contrary to pathological processes, normal aging primarily affects septohippocampal projections instead of those arising from the NBM or pontine nuclei.

Overall, this aging-related alteration supports specific cholinergic vulnerability linked to the aging process. Such vulnerability possibly represents a neurodegenerative phenomenon amenable to neuroprotective treatments. However, much remains to be determined the exact nature of this observation.

In conclusion, our results indicate that PET [^{18}F]FEOBV is a sensitive method to quantify neocortical and allocortical presynaptic cholinergic terminals in the living brain. [^{18}F]FEOBV demonstrates losses of cholinergic terminals induced by lesions or physiological processes like aging. PET imaging of VAcHT with [^{18}F]FEOBV represents a promising method for the quantification of presynaptic cholinergic deficits in human diseases.

CONCLUSION

Les résultats de ce travail ont permis notamment de répliquer d'autres données montrant que la distribution cérébrale du [^{18}F]FEOBV est conforme aux connaissances actuelles sur la neuroanatomie des projections cholinergiques dans le SNC (Landry St-Pierre *et al.*, 2008a ; Mulholland *et al.*, 1998). La plus grande concentration de [^{18}F]FEOBV a été observée dans le striatum, très riche en interneurons cholinergiques (Mesulam *et al.*, 1992). De fortes concentrations ont également été détectées dans le cortex frontal et le thalamus, qui reçoivent respectivement les projections les plus denses du NBM et celles des noyaux cholinergiques du tronc cérébral (NTPP et NTLD) (Mesulam *et al.*, 1989 ; Mesulam *et al.*, 1983). Ces résultats suggèrent une bonne fiabilité du [^{18}F]FEOBV pour marquer les sites de projection cholinergiques du SNC.

Les résultats obtenus à la suite d'une lésion expérimentale unilatérale du NBM sont plus novateurs. Ils montrent d'abord la sensibilité du [^{18}F]FEOBV pour détecter des changements induits aux systèmes cholinergiques. De plus, puisque la lésion cholinergique induite est analogue à celles observées dans la MA, le [^{18}F]FEOBV pourrait être un outil prometteur pour l'identification, l'évaluation et le suivi thérapeutique de la MA. En d'autres mots, il semble possible que le [^{18}F]FEOBV puisse servir de marqueur biologique de la MA, un outil diagnostique qui fait présentement défaut. La possibilité de détecter la présence ou l'absence d'une lésion cholinergique constitue donc un bon départ, mais il reste encore à démontrer la sensibilité de ce marqueur. Des études ultérieures pourraient s'intéresser, par exemple, à induire différents degrés de lésions cholinergiques, pour vérifier si les valeurs de liaison du [^{18}F]FEOBV montrent une corrélation avec d'autres marqueur

fiables, tel que le comptage *post-mortem* de marqueurs immunohistochimiques des cellules cholinergiques.

Un autre résultat intéressant, bien qu'inattendu, est l'observation d'une réduction significative de [¹⁸F]FEOBV dans l'hémisphère controlatéral à la lésion. Cela pourrait suggérer des projections encore mal connues du NBM vers le cortex controlatéral. Cette notion est particulièrement pertinente si l'on considère les quelques études ayant utilisé la saporine-IgG 192 unilatéralement (par exemple : Wenk, et al., 2004), qui ont analysé l'hémisphère controlatérale comme contrôle, prenant apparemment pour acquis que la lésion reste unilatérale. Des études plus systématiques devront être effectuées pour explorer cette question qui relève d'avantage de la neuroanatomie.

L'effet observé chez les rats âgés supporte également le potentiel du [¹⁸F]FEOBV à détecter *in vivo* des altérations cérébrales cholinergiques. La diminution la plus notable ayant été localisée dans les hippocampes plutôt que généralisée dans l'ensemble au cortex, il semble que la diminution des fibres cholinergiques associée au vieillissement normal pourrait être différente de celle associée aux troubles neurodégénératifs. Ce serait ainsi les projections aux hippocampes, provenant du septum médian, qui serait plus vulnérables dans le cas du vieillissement normal, plutôt que celles reliant le NBM au cortex.

Pour conclure, le [¹⁸F]FEOBV est tout au moins être assez sensible pour détecter de manière discriminante deux altérations des systèmes cholinergiques, aux niveaux néo- et allocortical. Jusqu'ici, le [¹⁸F]FEOBV semble donc prometteur comme outil d'évaluation *in vivo* de l'intégrité des neurones cholinergiques.

APPENDICE A: FIGURES

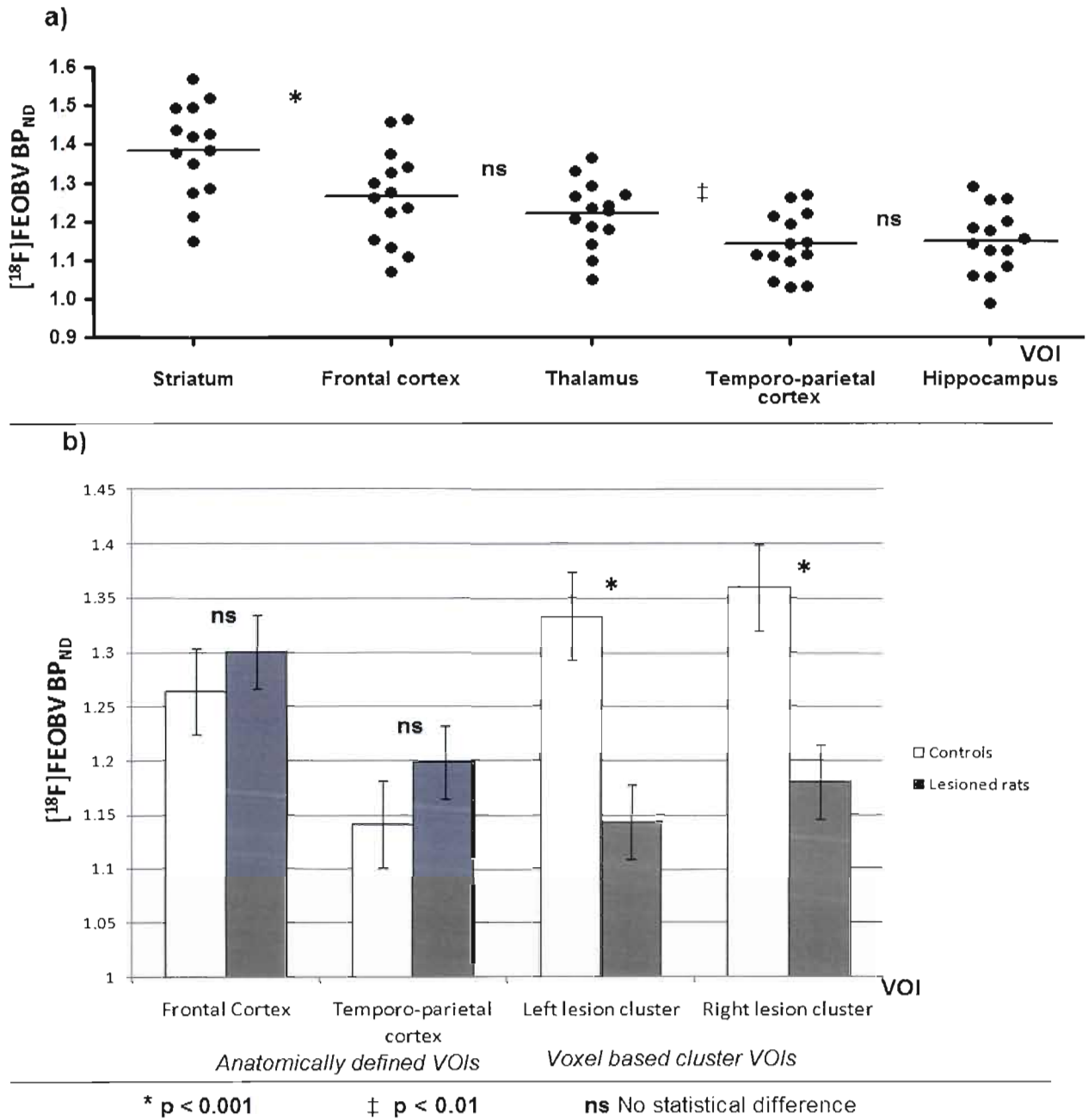


Figure 1: [¹⁸F]FEOBV distribution in controls (a) and regional effect of NBM lesions (b).

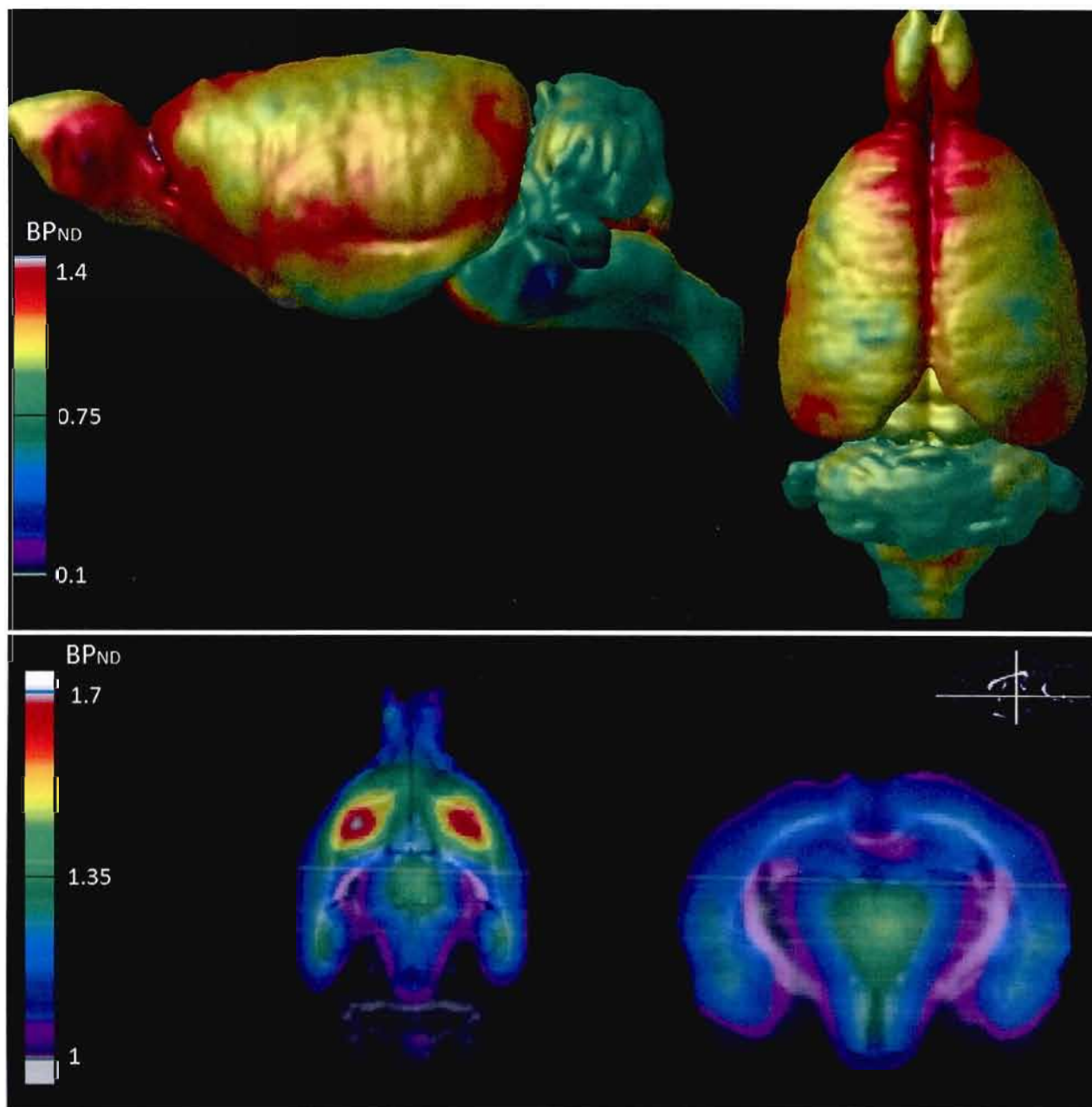


Figure 2: Average [^{18}F]FEOBV BP_{ND} maps in 7 young normal rats. Images projected on the brain surfaces (top) and transectional volumes (bottom).

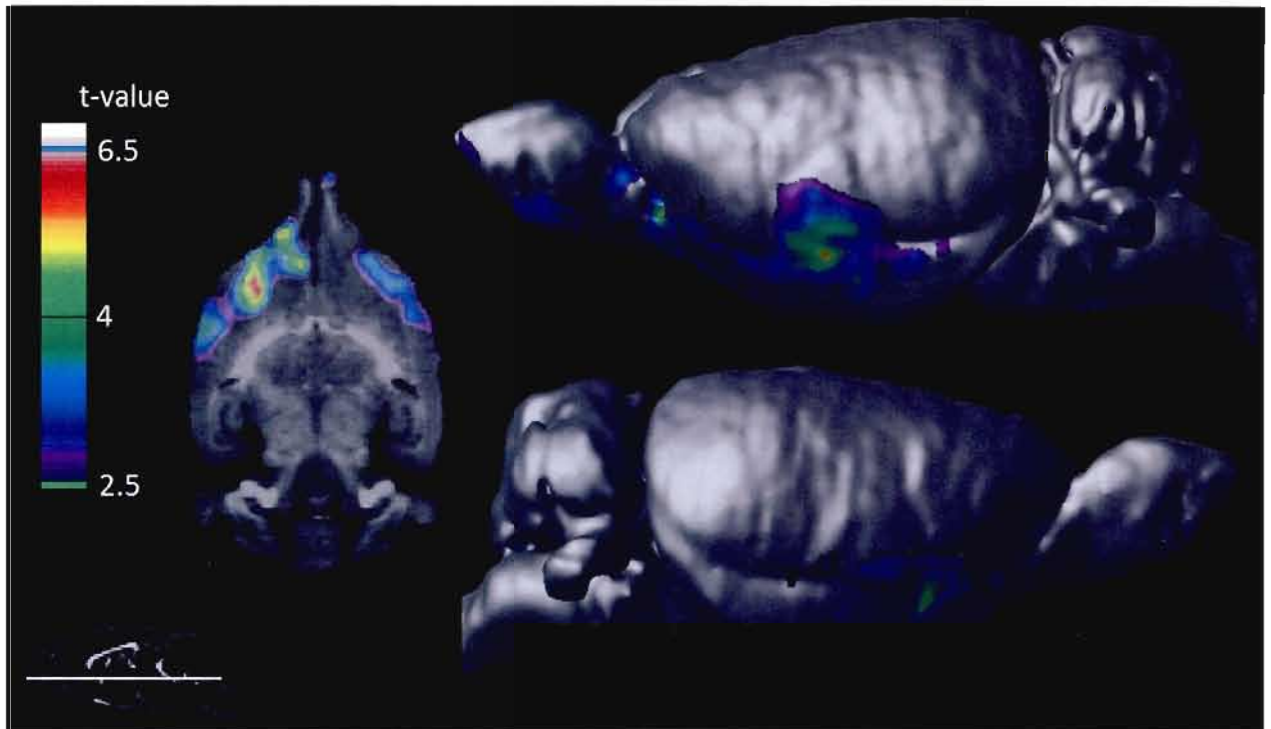


Figure 3: t-statistical maps [non-lesioned > NBM lesioned] representing cortical declines of the $[^{18}\text{F}]\text{FEOBV BP}_{\text{ND}}$ following NBM lesion. Images projected on the brain surface and transectional volumes.

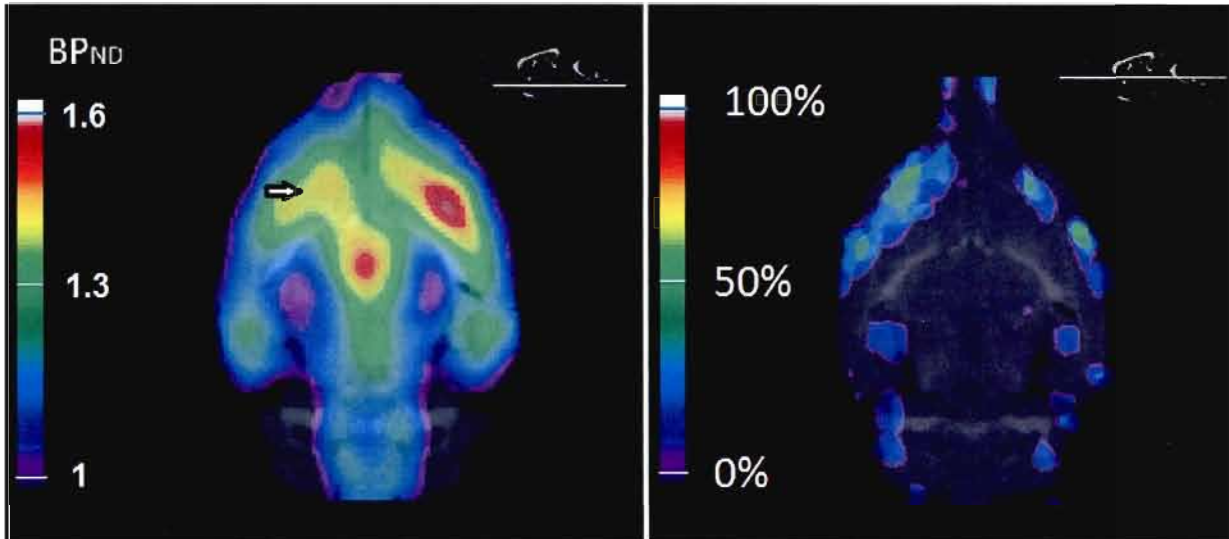


Figure 4: Distribution of $[^{18}\text{F}]\text{FEOBV } BP_{ND}$ declines following lesion of the NBM. BP_{ND} images overlay on histological template (left) shows decline of average binding following a NBM lesion in the left hemisphere (arrow). Probabilistic (right) images show large variability as well as the greatest effect in the ipsilateral frontal area.

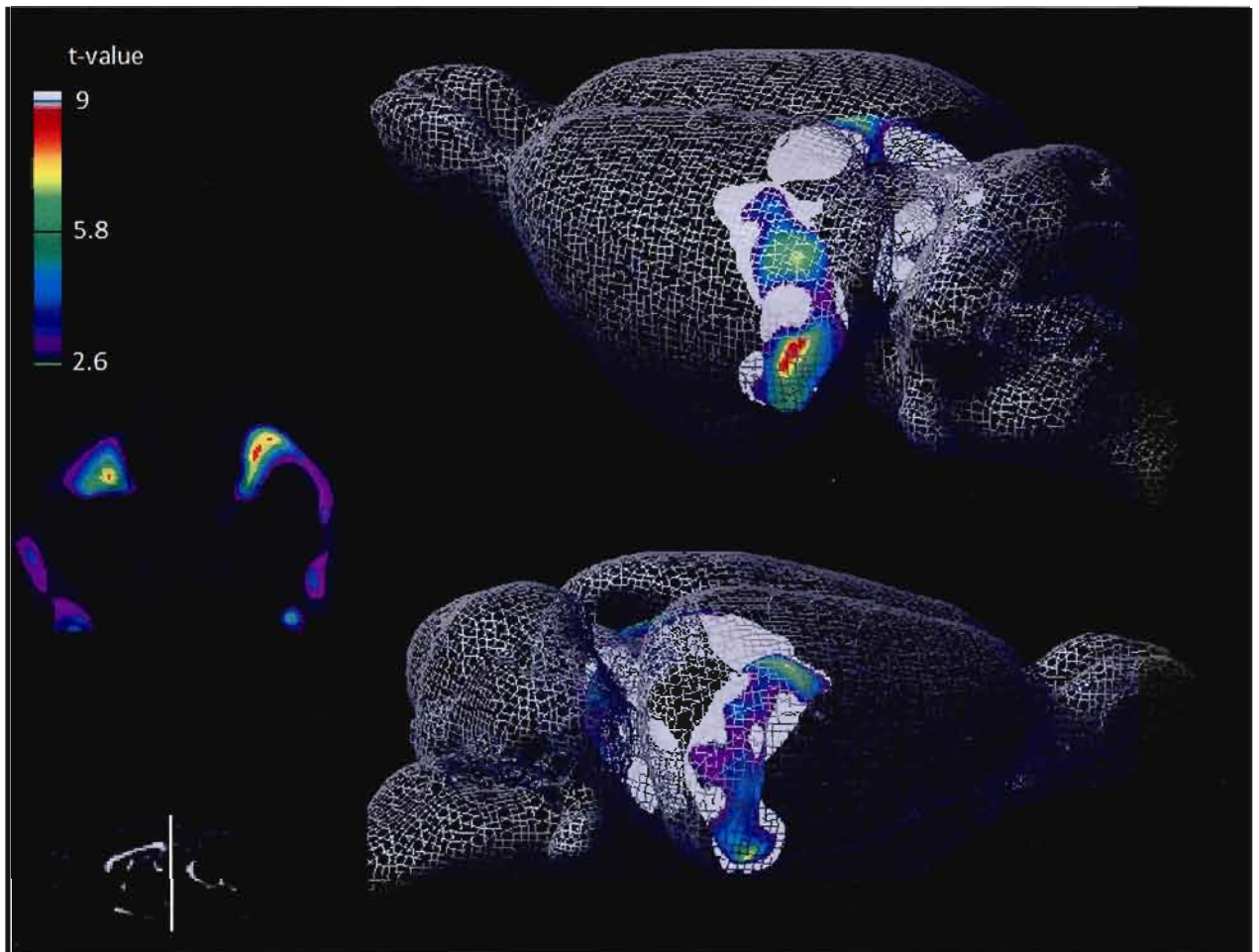


Figure 5: t-statistical maps [3 months > 18 months old rats] representing declines of $[^{18}\text{F}]$ FEOBV BP_{ND} in the old rats projected on the brain surface and volume.

RÉFÉRENCES

- Canas, P. M., J. M. Duarte, R. J. Rodrigues, A. Kofalvi et R. A. Cunha. 2009. «Modification upon aging of the density of presynaptic modulation systems in the hippocampus». *Neurobiol Aging*, vol. 30, no 11, p. 1877-1884
- Dickson, D. W., H. A. Crystal, C. Bevona, W. Honer, I. Vincent et P. Davies. 1995. «Correlations of synaptic and pathological markers with cognition of the elderly». *Neurobiol Aging*, vol. 16, no 3, p. 285-298; discussion 298-304
- Dournaud, P., P. Delaere, J. J. Hauw et J. Epelbaum. 1995. «Differential correlation between neurochemical deficits, neuropathology, and cognitive status in Alzheimer's disease». *Neurobiol Aging*, vol. 16, no 5, p. 817-823
- Efange, S. M. 2000. «In vivo imaging of the vesicular acetylcholine transporter and the vesicular monoamine transporter». *FASEB J*, vol. 14, no 15, p. 2401-2413
- Everitt, B. J., et T. W. Robbins. 1997. «Central cholinergic systems and cognition». *Annu Rev Psychol*, vol. 48, p. 649-684
- Fuhrmann, G., T. Durkin, G. Thiriet, E. Kempf et A. Ebel. 1985. «Cholinergic neurotransmission in the central nervous system of the Snell dwarf mouse». *J Neurosci Res*, vol. 13, no 3, p. 417-430
- Giboureau, N., P. Emond, R. R. Fulton, D. J. Henderson, S. Chalon, L. Garreau, P. Roselt, S. Eberl, S. Mavel, S. Bodard, M. J. Fulham, D. Guilloteau et M. Kassiou. 2007. «Ex vivo and in vivo evaluation of (2R,3R)-5-[(18)F]-fluoroethoxy- and fluoropropoxy-benzovesamicol, as PET radioligands for the vesicular acetylcholine transporter». *Synapse*, vol. 61, no 12, p. 962-970
- Giboureau, N., I. M. Som, A. Boucher-Arnold, D. Guilloteau et M. Kassiou. 2010. «PET radioligands for the vesicular acetylcholine transporter (VAChT)». *Curr Top Med Chem*, vol. 10, no 15, p. 1569-1583

- Gilmor, M. L., N. R. Nash, A. Roghani, R. H. Edwards, H. Yi, S. M. Hersch et A. I. Levey. 1996. «Expression of the putative vesicular acetylcholine transporter in rat brain and localization in cholinergic synaptic vesicles». *J Neurosci*, vol. 16, no 7, p. 2179-2190
- Henderson, J. M., K. Carpenter, H. Cartwright et G. M. Halliday. 2000. «Loss of thalamic intralaminar nuclei in progressive supranuclear palsy and Parkinson's disease: clinical and therapeutic implications». *Brain*, vol. 123 (Pt 7), p. 1410-1421
- Hirano, S., H. Shinotoh, H. Shimada, A. Aotsuka, N. Tanaka, T. Ota, K. Sato, H. Ito, S. Kuwabara, K. Fukushi, T. Irie et T. Suhara. 2010. «Cholinergic imaging in corticobasal syndrome, progressive supranuclear palsy and frontotemporal dementia». *Brain*, vol. 133, no Pt 7, p. 2058-2068
- Ichikawa, T., K. Ajiki, J. Matsuura et H. Misawa. 1997. «Localization of two cholinergic markers, choline acetyltransferase and vesicular acetylcholine transporter in the central nervous system of the rat: in situ hybridization histochemistry and immunohistochemistry». *J Chem Neuroanat*, vol. 13, no 1, p. 23-39
- Innis, R. B., V. J. Cunningham, J. Delforge, M. Fujita, A. Gjedde, R. N. Gunn, J. Holden, S. Houle, S. C. Huang, M. Ichise, H. Iida, H. Ito, Y. Kimura, R. A. Koeppe, G. M. Knudsen, J. Knuuti, A. A. Lammertsma, M. Laruelle, J. Logan, R. P. Maguire, M. A. Mintun, E. D. Morris, R. Parsey, J. C. Price, M. Slifstein, V. Sossi, T. Suhara, J. R. Votaw, D. F. Wong et R. E. Carson. 2007. «Consensus nomenclature for in vivo imaging of reversibly binding radioligands». *J Cereb Blood Flow Metab*, vol. 27, no 9, p. 1533-1539
- Kilbourn, M. R., B. Hockley, L. Lee, P. Sherman, C. Quesada, K. A. Frey et R. A. Koeppe. 2009. «Positron emission tomography imaging of (2R,3R)-5-[(18F]fluoroethoxybenzovesamicol in rat and monkey brain: a radioligand for the vesicular acetylcholine transporter». *Nucl Med Biol*, vol. 36, no 5, p. 489-493
- Kovalenko, N. Y., et D. D. Matsievskii. 2005. «Role of cholinergic structures in individual resistance of rat circulatory system to posthemorrhagic hypoxia». *Bull Exp Biol Med*, vol. 140, no 2, p. 177-180
- Landry St-Pierre, E., P. Rosa Neto, G. Massarweh, A. Aliaga, S. Mzengeza, M. A. Bedard et J-P. Soucy. 2008a. «Distribution of [18F]-FEOBV in rat: a

promising tracer for imaging cholinergic innervation densities.». *Can J Neurol Sci*, vol. 35, no 1, p. S46

- Landry St-Pierre, E., P. Rosa Neto, G. Massarweh, A. Aliaga, S. Mzengeza, M. A. Bedard et J-P. Soucy. 2008b. «Plasma chromatographic profile of [18F]-FEOBV in rat: results and implications for clinical applications. ». *Can J Neurol Sci*, vol. 35, no 1, p. S46-S47
- Levin, E. D., et B. B. Simon. 1998. «Nicotinic acetylcholine involvement in cognitive function in animals». *Psychopharmacology (Berl)*, vol. 138, no 3-4, p. 217-230
- Logan, J., J. S. Fowler, N. D. Volkow, A. P. Wolf, S. L. Dewey, D. J. Schlyer, R. R. MacGregor, R. Hitzemann, B. Bendriem, S. J. Gatley et al. 1990. «Graphical analysis of reversible radioligand binding from time-activity measurements applied to [N-11C-methyl]-(-)-cocaine PET studies in human subjects». *J Cereb Blood Flow Metab*, vol. 10, no 5, p. 740-747
- Mazere, J., C. Prunier, O. Barret, M. Guyot, C. Hommet, D. Guilloteau, J. F. Dartigues, S. Auriacombe, C. Fabrigoule et M. Allard. 2008. «In vivo SPECT imaging of vesicular acetylcholine transporter using [(123)I]-IBVM in early Alzheimer's disease». *Neuroimage*, vol. 40, no 1, p. 280-288
- McGaughy, J., J. W. Dalley, C. H. Morrison, B. J. Everitt et T. W. Robbins. 2002. «Selective behavioral and neurochemical effects of cholinergic lesions produced by intrabasal infusions of 192 IgG-saporin on attentional performance in a five-choice serial reaction time task». *J Neurosci*, vol. 22, no 5, p. 1905-1913
- Mesulam, M. M., et C. Geula. 1988. «Nucleus basalis (Ch4) and cortical cholinergic innervation in the human brain: observations based on the distribution of acetylcholinesterase and choline acetyltransferase». *J Comp Neurol*, vol. 275, no 2, p. 216-240
- Mesulam, M. M., C. Geula, M. A. Bothwell et L. B. Hersh. 1989. «Human reticular formation: cholinergic neurons of the pedunclopontine and laterodorsal tegmental nuclei and some cytochemical comparisons to forebrain cholinergic neurons». *J Comp Neurol*, vol. 283, no 4, p. 611-633
- Mesulam, M. M., D. Mash, L. Hersh, M. Bothwell et C. Geula. 1992. «Cholinergic innervation of the human striatum, globus pallidus, subthalamic nucleus, substantia nigra, and red nucleus». *J Comp Neurol*, vol. 323, no 2, p. 252-268

- Mesulam, M. M., E. J. Mufson, A. I. Levey et B. H. Wainer. 1983. «Cholinergic innervation of cortex by the basal forebrain: cytochemistry and cortical connections of the septal area, diagonal band nuclei, nucleus basalis (substantia innominata), and hypothalamus in the rhesus monkey». *J Comp Neurol*, vol. 214, no 2, p. 170-197
- Mufson, E. J., S. E. Counts, S. E. Perez et S. D. Ginsberg. 2008. «Cholinergic system during the progression of Alzheimer's disease: therapeutic implications». *Expert Rev Neurother*, vol. 8, no 11, p. 1703-1718
- Muir, J. L., B. J. Everitt et T. W. Robbins. 1994. «AMPA-induced excitotoxic lesions of the basal forebrain: a significant role for the cortical cholinergic system in attentional function». *J Neurosci*, vol. 14, no 4, p. 2313-2326
- Muir, J. L., K. J. Page, D. J. Sirinathsinghji, T. W. Robbins et B. J. Everitt. 1993. «Excitotoxic lesions of basal forebrain cholinergic neurons: effects on learning, memory and attention». *Behav Brain Res*, vol. 57, no 2, p. 123-131
- Mulholland, G. K., D. M. Wieland, M. R. Kilbourn, K. A. Frey, P. S. Sherman, J. E. Carey et D. E. Kuhl. 1998. «[18F]fluoroethoxy-benzovesamicol, a PET radiotracer for the vesicular acetylcholine transporter and cholinergic synapses». *Synapse*, vol. 30, no 3, p. 263-274
- Mzengeza, S., G. Massarweh, P. Rosa Neto, J-P. Soucy et M. A. Bedard. 2007. «Radiosynthesis of [18F]FEOV and in vivo PET imaging of acetylcholine vesicular transporter in the rat». *J Cereb Blood Flow Metab*, vol. 27, no 1S, p. 10-17U
- Olmstead, M. C., et K. B. Franklin. 1993. «Effects of pedunculo-pontine tegmental nucleus lesions on morphine-induced conditioned place preference and analgesia in the formalin test». *Neuroscience*, vol. 57, no 2, p. 411-418
- Paxinos, G., et C. Watson. 2009. *The Rat Brain in Stereotaxic Coordinates, 6th ed.* . Academic Press, San Diego: p.
- Pizzo, D. P., J. J. Waite, L. J. Thal et J. Winkler. 1999. «Intraparenchymal infusions of 192 IgG-saporin: development of a method for selective and discrete lesioning of cholinergic basal forebrain nuclei». *J Neurosci Methods*, vol. 91, no 1-2, p. 9-19

- Podruchny, T. A., C. Connolly, A. Bokde, P. Herscovitch, W. C. Eckelman, D. O. Kiesewetter, T. Sunderland, R. E. Carson et R. M. Cohen. 2003. «In vivo muscarinic 2 receptor imaging in cognitively normal young and older volunteers». *Synapse*, vol. 48, no 1, p. 39-44
- Prohovnik, I., D. P. Perl, K. L. Davis, L. Libow, G. Lesser et V. Haroutunian. 2006. «Dissociation of neuropathology from severity of dementia in late-onset Alzheimer disease». *Neurology*, vol. 66, no 1, p. 49-55
- Quirion, R. 1993. «Cholinergic markers in Alzheimer disease and the autoregulation of acetylcholine release». *J Psychiatry Neurosci*, vol. 18, no 5, p. 226-234
- Risbrough, V., B. Bontempi et F. Menzagli. 2002. «Selective immunolesioning of the basal forebrain cholinergic neurons in rats: effect on attention using the 5-choice serial reaction time task». *Psychopharmacology (Berl)*, vol. 164, no 1, p. 71-81
- Rubins, D. J., W. P. Melega, G. Lacan, B. Way, A. Plenevaux, A. Luxen et S. R. Cherry. 2003. «Development and evaluation of an automated atlas-based image analysis method for microPET studies of the rat brain». *Neuroimage*, vol. 20, no 4, p. 2100-2118
- Sherman, K. A., et E. Friedman. 1990. «Pre- and post-synaptic cholinergic dysfunction in aged rodent brain regions: new findings and an interpretative review». *Int J Dev Neurosci*, vol. 8, no 6, p. 689-708
- Soucy, J-P., P. Rosa Neto, G. Massarweh, A. Aliaga, E. Schirrmacher, M. A. Bedard, M. Sanchez-Legaspi, P. Gravel et A. Reader. 2010. «Imaging of cholinergic terminals in the non-human primate brain using 18F-FEOBV PET : Development of a tool to assess cholinergic losses in Alzheimer's disease.». *Alzheimer Dis Assoc Disord*, vol. 6, p. S-286
- Szymusiak, R. 1995. «Magnocellular nuclei of the basal forebrain: substrates of sleep and arousal regulation». *Sleep*, vol. 18, no 6, p. 478-500
- Thal, L. J., K. Kantarci, E. M. Reiman, W. E. Klunk, M. W. Weiner, H. Zetterberg, D. Galasko, D. Pratico, S. Griffin, D. Schenk et E. Siemers. 2006. «The role of biomarkers in clinical trials for Alzheimer disease». *Alzheimer Dis Assoc Disord*, vol. 20, no 1, p. 6-15
- Voytko, M. L. 1996. «Cognitive functions of the basal forebrain cholinergic system in monkeys: memory or attention?». *Behav Brain Res*, vol. 75, no 1-2, p. 13-25

- Ward, M. 2007. «Biomarkers for Alzheimer's disease». *Expert Rev Mol Diagn*, vol. 7, no 5, p. 635-646
- Weihe, E., J. H. Tao-Cheng, M. K. Schafer, J. D. Erickson et L. E. Eiden. 1996. «Visualization of the vesicular acetylcholine transporter in cholinergic nerve terminals and its targeting to a specific population of small synaptic vesicles». *Proc Natl Acad Sci U S A*, vol. 93, no 8, p. 3547-3552
- Wenk, G. L., J. D. Stoehr, G. Quintana, S. Mobley et R. G. Wiley. 1994. «Behavioral, biochemical, histological, and electrophysiological effects of 192 IgG-saporin injections into the basal forebrain of rats». *J Neurosci*, vol. 14, no 10, p. 5986-5995
- Whitehouse, P. J., J. C. Hedreen, C. L. White, 3rd et D. L. Price. 1983. «Basal forebrain neurons in the dementia of Parkinson disease». *Ann Neurol*, vol. 13, no 3, p. 243-248
- Whitehouse, P. J., D. L. Price, R. G. Struble, A. W. Clark, J. T. Coyle et M. R. Delon. 1982. «Alzheimer's disease and senile dementia: loss of neurons in the basal forebrain». *Science*, vol. 215, no 4537, p. 1237-1239
- Ypsilanti, A. R., M. T. Girao da Cruz, A. Burgess et I. Aubert. 2008. «The length of hippocampal cholinergic fibers is reduced in the aging brain». *Neurobiol Aging*, vol. 29, no 11, p. 1666-1679